Mechanical properties of PTMC scaffolds constructed by Stereolithography for the repair of Annulus Fibrosus tissue. Effect of scaffold characteristics on cell adhesion and proliferation

Ana Luísa Parruca da Cruz

October 2014 | Instituto Superior Técnico, Lisboa, Portugal

analuisapc@tecnico.ulisboa.pt | a.l.parrucadacruz@student.utwente.nl

Abstract

Degeneration of the intervertebral disc affects around 97 *%* of individuals 50 years or older in a worldwide scale and is known to prompt cases of chronic low back pain as well as some related pathologies, such as disc herniation. Current treatment options are costly, invasive and relatively ineffective, being solely based on pain management and lacking capability of rehabilitation of the bio-mechanical characteristics of disc structure. Furthermore, outcomes are limited when it comes to disc functionality and can lead to further degeneration. As an alternative, tissue engineering strategies are being developed in hope to regain total disc functionality. Regeneration of the outer layer of the disc, the *annulus fibrosus*, is the most challenging because of its complex organization. In the current project we optimize the design characteristics of a previously developed gyroid architecture PTMC scaffold built by stereolithography for repair of the AF tissue. Scaffolds seeded with human *annulus fibrosus* cells displayed excellent cell adhesion and distribution. Higher rates of cell proliferation were observed for higher pore sizes (493 *μm*) and porosities (≥ 67 *%*). When regarding mechanical properties, scaffolds with a pore size of 400 *μm* and 70 *%* porosity, showed an increase of two times their initial value of compression modulus, after 14 days of culture reaching a value of 0.609±0.215 MPa comparable to that of native human AF tissue. PTMC built scaffolds exhibit promising bio-mechanical properties, increasing its relevance when constructing functional AF replacements.

Key words: Intervertebral Disc; Disc Degeneration; Annulus Fibrosus Regeneration; Bio-mechanical characteristics; Poly-(trimethylene carbonate); Scaffold Design

1 Introduction

The intervertebral disc (IVD) is a complex structure formed by a semi-cartilaginous tissue, located in the vertebral column between the cartilage endplates of the column's vertebrae [3]. It is responsible for movements like flexion, bending and torsion of the spine, and also the bearing of loads and forces of impact [4], [5].

The IVD can be differentiated into two different anatomical zones, the *nucleus pulposus* and the *annulus fibrosus* [3], [6]. The *nucleus pulposus* (NP) is the core of the IVD and is composed by a highly hydrated gelatinous and homogeneous mass [3], [4], that possesses a viscoelastic behaviour that allows its structure to expand under compressive forces [3], [7]. Surrounding the NP is the *annulus fibrosus* (AF), a lamellar and fibrocartilaginous structure, which is built to resist large and compound loads that arise during physiologic joint movements [7]. The AF prevents the NP from leaking and maintains the IVD in place [5]. The several concentric lamellae that compose the AF are composed by highly oriented and organized collagen fibres, mainly type I [8], inserted in a non-fibrilar hydrated network of proteoglycans [9]. Elastin fibres are interlaced among the collagen, allowing the disc to

return to its initial location after movement. AF cells are considered fibrochondrocytes [4], and they are present in a density two times greater than the NP tissue, about $9 \cdot 10^6$ *cells/cm³* in mature healthy subjects [5], [8].

Normal production of extracellular matrix is essential for a healthy IVD. Degeneration or aging of the IVD tissue, leads to loss of disc height and hydration of the NP tissue, placing more pressure on the fibres of the AF, which can tear, enabling the leakage of the NP and hernia formation [5] [10]. Nevertheless disc herniation and other pathologies can also be caused by traumatic events where damaging forces are applied, inflammation of the IVD structure [4] or progression of disc degeneration [11].

Low back pain (LBP) is associated with several spinal pathologies [4], and its occurrence varies from person to person, according to the subject's age, health, bone mass index, strength of the abdominal and back muscles. Routine habits such as smoking or the bearing of heavy loads [4],[11], may reduce the availability of blood in the tissue, hindering the supply of nutrients and consequently decreasing cell activity and viability [4], progressing or initiating the degeneration process [11]. The AF has low self-regenerating capabilities and the healing process is usually characterized by the production of new connective tissue, complemented with neovascularization, ingrowth of nerve fibres [10] and sometimes ingrowth of bony outgrowths [4]. Low back pain is mostly presented in advanced stages of the degeneration, when the AF is affected and in which the whole IVD structure is already altered [4].

Currently, a great variety of treatment options for disc related conditions are available, however these are more focussed on mitigating the symptoms than treating the source of the pain. Surgical treatments range from lumbar discectomy and/or spinal fusion, disc arthroplasty and dynamic stabilization to some minimal invasive methodologies. However these usually present several disadvantages, like reduction of the patient's column flexibility, need for follow-up surgeries, recurrent herniation, decrease of disc height, increase of stress in adjacent vertebrae and most of the times amplified and persisting LBP [4], [10].

Low back pain and disc degeneration have a massive detrimental impact on modern's society, from a social, economic and medical point of view [4], affecting the working and elderly population [4], [8]. In the USA, medical and absence related costs reach US$100 bilion [1]. Besides high lifetime prevalence situated between 58*%* and 84*%* [4], patients with LBP commonly require extended times of bed rest. All these factors contribute for the importance of finding a solution that can provide better patient outcomes. Tissue engineering techniques are evolving with the objective of developing a solution that not only diminishes the pain felt by the patient, but also restores the intrinsic properties and functionalities of the disc [4]. In the past decade research has been focused on NP regeneration [8], however closure of the complex surrounding *annulus fibrosus* tissue is still the main challenge [11].

Engineered AF has to support pressurization of the NP, stand the loads created by torsion and bending of the spine and provide a quick closure of the defect [3], [8], [10]. A wide range of construction methods, architectures and materials have been studied. One of the first types of materials considered for AF repair were hydrogels. These are biocompatible, immunologically tolerated and easy to apply, however they lack the needed mechanical properties, not being able to sustain the stress and shear of the AF [12], [13]. Furthermore previous work showed that with culture time some hydrogels change the AF's cells phenotype [4] [5]. More recently electrospun scaffolds have been constructed in the hope to mimic the native AF lamellar structure [14], [15], [16], [17]. Several materials have been used from silk [3], [18], poly(Ɛ-caprolactone), to polycarbonate urethane [15], among others. Even though structural hierarchy of the AF was achieved, mechanical stiffness of the constructs didn't match those of native IVD. Additionally constructs commonly presented low cell infiltration and distribution [14], [16], [9], [19], [20].

Application of stereolithography (SL) is relatively new in the field of AF tissue engineering, but has presented good outcomes in previous studies [2], [6], [21], allowing specific control of the construct's properties and construction of tailor-made scaffolds. In previous studies, porous PTMC gyroid scaffolds prepared by SL demonstrated not only good cell infiltration and proliferation but also high compression modulus in the dry state [2]. Pore sizes of 230 μm (0.31±0.09 MPa [2]) presented compression modulus in the range of the

reported in the literature for AF tissue (0.21±0.13 MPa to 0.56±0.21 MPa) [2], [10], proving to be appropriate for AF repair. Moreover the synthetic polymer PTMC possesses intrinsically suitable mechanical properties, being also biocompatible and biodegradable by enzymatic surface degradation with non-toxic and non-acidic degradation products.

In the current project we aim to optimize the design parameters of a PTMC scaffold built using stereolithography for AF repair, constructed with a gyroid architecture and seeded with human *annulus fib*rosus cells (hAFC). Moreover, the effect of culture time (up to 14 days) on the mechanical properties of the porous scaffolds will be assessed by compression tests. Design parameters are not independent of each other, so different experiments of constant surface area and constant pore size were performed to assess the effect of pore size and porosity, respectively (Table 1). Cell adhesion, proliferation and distribution were investigated performing a Methylene Blue staining after 24 hours, 7 days and 14 days of culture. Cell Viability was assessed using a Live/Dead® assay.

Table 1 Design characteristics of the scaffolds used for the constant surface area [1], constant pore size [2] and mechanical testing [3] experiments.

Pore size (μm)	Porosity (%)	Number of pores	Specific Surface Area (μm^{-1})	Experiment
311	62.0	8	7.00	[1]
383	69.0	7		
493	74,7	6		
430	57.0	6	4.66	[2]
	67.0	.	7.36	
	77.0	10	16.52	
400	70.0	6	6.27	[3]

2 Materials and Methods

2.1 Preparation of the PTMC scaffolds

The PTMC resin was prepared in a two-step reaction. On the first step a hydroxyl-ended PTMC oligomer was prepared by ring-opening polymerization of 1,3-trimethylene carbonate (TMC Foryou Medical®, China), initiated by tri(hydroxymethyl) propane (TMP Sigma Aldrich® Netherlands) and catalysed by $Sn(Oct)_2$ (0.05 *wt%*; Sigma Aldrich® Netherlands) was used. The polymerization was carried-out in an argon protected atmosphere for a total of 3 days at 130 *°C*. The resulting oligomer was end-functionalized with methacrylate groups by a 2 days reaction at 120 *°C* with methacrylic anhydride (94 *%*; Sigma Aldrich® Netherlands) at an excess of 50 *mol%* [2] [22]. The resin was purified using a vacuum distillation at a maximum temperature of 130 *°C* [22]. The degree of functionalization, rate of conversion and monomer molecular weight were determined by ^1H NMR spectroscopy (Varian Innova® 300 *MHz*, USA).

The PTMC resin was prepared by dilution of 5000 *g/mol* in propylene carbonate. Lucirin TPO-L (5 *%wt*) and Orasol Orange dye (0.15 *wt%*) were added to resin, a photo-initiator and a dye for control of the penetration depth, respectively. The photo-polymerization was performed layer-by-layer using an EnvisionTech Perfactory MiniMultilens stereolithography apparatus using a blue light (400-500 *nm*). The layer thickness was 25 μm at a pixel resolution of 16·16 μm^2, the illumination time for layer was 40 seconds with an intensity of 20 mW/cm^2 [2]. The resulting scaffolds were extracted in acetone and dried, until a constant value of weight was reached. Each scaffold is approximately 5 mm^2, considering a 15 *%* of shrinkage. Sterilization was performed by placing the scaffolds in ethanol for 30 minutes. Constructs were washed with DPBS and kept in NPCM medium overnight previous to seeding.

2.2 Scaffold Characterization

In order to determine the network characteristics of the built scaffolds, a micro-computed tomography was performed using a eXplore Locus GE µ-CT scanner with a resolution of 8 μm (General Electric®, USA).

2.3 Cell culturing and seeding

Human *annulus fibrosus* cells (passage 3; Science Cell, USA) where thawed and expanded using an expansion medium, consisting in a Nucleus

Pulposus Culture Medium (NPCM, Science Cell® USA) supplemented with 2*%* Fetal Bovine Serum, 1 *%* Nucleus Pulposus Cell Growth Supplement and 1 % of a Penicillin/Streptomycin antibiotic solution, all obtained from Science Cell®, USA. Each scaffold was seeded from the top by pipetting a total of 200 000 passage 4 cells, present on a volume of 100 *µL* of cell suspension. The seeding was carried out in a 24 well-plate, and the drained cell suspension was reapplied to the top of the scaffold 3 times. The scaffolds were incubated for 3 hours, after this period 1 *mL* of medium was added. Constructs were kept under static culture conditions in a humidified air incubator from *SANYO*, with 5 *%* CO_2 at 37 *°C*. Medium refreshments of 1 *mL* took place every other day.

Histological, mechanical and other analysis were preformed after 24 hours, 7 days and 14 days of culture.

2.4 Microscopical and Histological Analyses

Cell's initial adhesion, proliferation and distribution were analysed performing a Methylene Blue staining. Samples were washed with Dulbecco's phosphate buffer solution (DPBS; Gilbco-BRL®, UK), fixed with a 3.7*%* solution of paraformaldehyde (PFA; Sigma-Aldrich®, Netherlands) and then stained, each with 4 drops of Loffler's methylene blue solution (LMBS; Sigma-Aldrich®, Netherlands). Specimens were imaged using a Nikon SM2-10A stereomicroscope equipped with a Sony 3CCD camera. Pictures of the bottom, top and cross-section of the scaffolds were taken with several magnifications

To assess cell viability and distribution, a Live/Dead® fluorescent staining (Invitrogen®, USA) was performed. Samples were rinsed with DPBS and then incubated for 35 minutes with a Live/Dead® working solution composed by EthD-1 and Calcein AM, with a concentration of 0.25 *µm* and 1.00 *µm*, respectively. Samples were visualized using an inverted fluorescence microscope (AMG®, ƐVOS *ft*) equipped with a Texas Red and a Green Fluorescent Protein filter. Viable cells were identified by its green fluorescence and the dead cells by a red fluorescence, samples were visualized from the top, bottom and cross-section.

2.5 DNA assay

The amount of cells present in each specimen was quantified using a CyQuant® proliferation assay. Non-adhering cells were washed-off using DPBS and the constructs were transferred into eppendorfs with 1 *mL* of 0.1 *%* Triton X-100 lysate buffer solution (Sigma-Aldrich®, Netherlands). Samples were hammered and frozen at -80 *°C* and then thawed, in a 2 times repeating cycle after which, the scaffold was removed and the samples centrifuged. Exactly 180 *µL* of CyQuant working solution, previously prepared with CyQuant GR® dye (400*x* diluted) and cell lysis buffer (20*x* diluted), using miliQ water as a solvent, was added to 20 *µL* of each sample's cell suspension. Fluorescence measurements were performed using a Tecan Safire 2 microplate reader, at an excitation maximum of 480 *nm* and emission maximum of 520 *nm*. Three samples (*n*=3) of each characteristic were analysed for each time-point.

2.6 Mechanical Testing

For the assessment of the mechanical properties of the scaffolds, compression tests were carried out at room temperature using a Zwick Z020 tensile tester armed with a 500 *N* load, data analysis and compression test details were specified using the *Xpert Series* II® software. Each scaffold was compressed until a maximum compression strain of 80 *%* was reached, at a constant velocity of 30 *%* strain per minute. Samples were compressed in a wet state and the compression moduli was determined between the values of 7 *%* and 9 *%* strain for all the samples, since for those the strain is linear dependent on the applied force.

2.7 Statistical analysis

Statistical analysis was performed using GraphPad Prism 5 software for Windows (GraphPad®, USA). For cell number Cy-Quant® assays, two-way analysis of variance, ANOVA, was executed. The different scaffolds were analysed and the behaviour of each in the 3 different time-points was compared using a Bonferroni post-test. For the compression tests a one-way ANOVA analysis was performed to analyse the evolution of the mean compression modulus. All the results considered significant were present within a set confidence interval of 95 *%*, which means that $P <$

0.050. The error reported in the figures corresponds to the standard deviation (SD).

3 Results

3.1 Cell Adhesion and Proliferation

Overall all scaffolds present an even distribution of the cells, which seem to have easily proliferated throughout the PTMC scaffolds. In both experiments there was an intensification of the staining over culture time, indicating that most of the scaffolds presented an increase in number of cells.

In the constant specific surface area experiment (7 μm^{-1}), results demonstrate that the seeding was efficient for the higher pore sizes (493 μm and 383 μm), providing a uniform cell distribution through the scaffold, however the smaller pore size scaffold (≤ 311 μm) presents a slightly uneven distribution of the cells on the first time-point (Figure 1). For the narrow pore scaffolds, the seeding technique employed was inefficient, mpst probably due to the use of static seeding conditions and scaffold's intrinsic PTMC hydrophobicity [(2), (21), (23)], which hinders the penetration of the cell seeding suspension.

With culture time there was an increasing difference in terms of cell proliferation between the scaffolds with different pore sizes with larger number of cells indicating higher proliferation for larger pore sizes (≥ 393 μm). After 14 days of culture the cells form tissue-like structures throughout the scaffolds, however only the 493 μm pore size scaffold, was completely and homogeneously filled with cells.

When assessing cell behaviour after 7 days of culture, one can observe that for the smaller pore sizes (311 μm) the proximity between pore's walls facilitates the lengthening of the cells to establish a connection between the different points on the structure. On the contrary, in larger pore scaffolds (493 μm), the cells first proliferated around the construct's backbone surface and only after started to fill the pores.

In the case of the experiment performed with constant pore size scaffolds (430 μm) with varying porosities, no problems related with cell seeding were observed. Also, cells present a similar behaviour in all the scaffolds, covering their structure first and only forming tissue-like structures after 7 days of culture.

The attained results suggest that porosities within the range of this study (57-77 %) had a minor influence on cell behaviour when compared to pore size, since larger pore sizes (430 μm), difficult the direct covering of the pores. Additionally the results were not completely conclusive, since constructs with higher porosities (67 *%* and 77 *%*) displayed comparable results and both appeared to be equally filled with cells, particularly after 7 and 14 days of culture. The lower porosity scaffold (57 *%*) presented an erratic behaviour, with a less clear evidence of an increase in cell number with culture time. Also, after 7 and 14 days of culture, was possible to observe the formation of cell aggregates on the bottom of the constructs, that presumably were a result of static culture in the well-plate and the scaffold's low porosity,

3.2 Cell Viability

The Live/Dead® staining revealed no dead cells at any time-point, meaning that the cells, even inside the scaffold, remained viable and had access to all the required nutrients and by products most probably didn't reach toxic levels. It was also possible to confirm and visualize with more precision, the previously reported behaviour and proliferation tendency of the cells. Nevertheless after 14 days of culture, deficient dye diffusion problems were evident, caused by the formation of tissue-like structures that started to cover the smaller pores (≤ 393 μm). Similar results were observed after 24 hours of seeding for the 311 μm pore size scaffold. This effect can become problematic overtime, as cell density increases, leading in extreme to nutrients and oxygen limitations. Likewise, analysis of the side of the scaffold with 311 μm pore size, indicates that after 14 days of culture, the cells had adhered to the culture well-plate and started to proliferate upwards to the sides of the scaffold, forming a thin layer of cells that covers the construct, clogging the pores, and aggravates nutrients and oxygen diffusion limitations into the interior, and toxic metabolites out, of the scaffold (Figure 2).

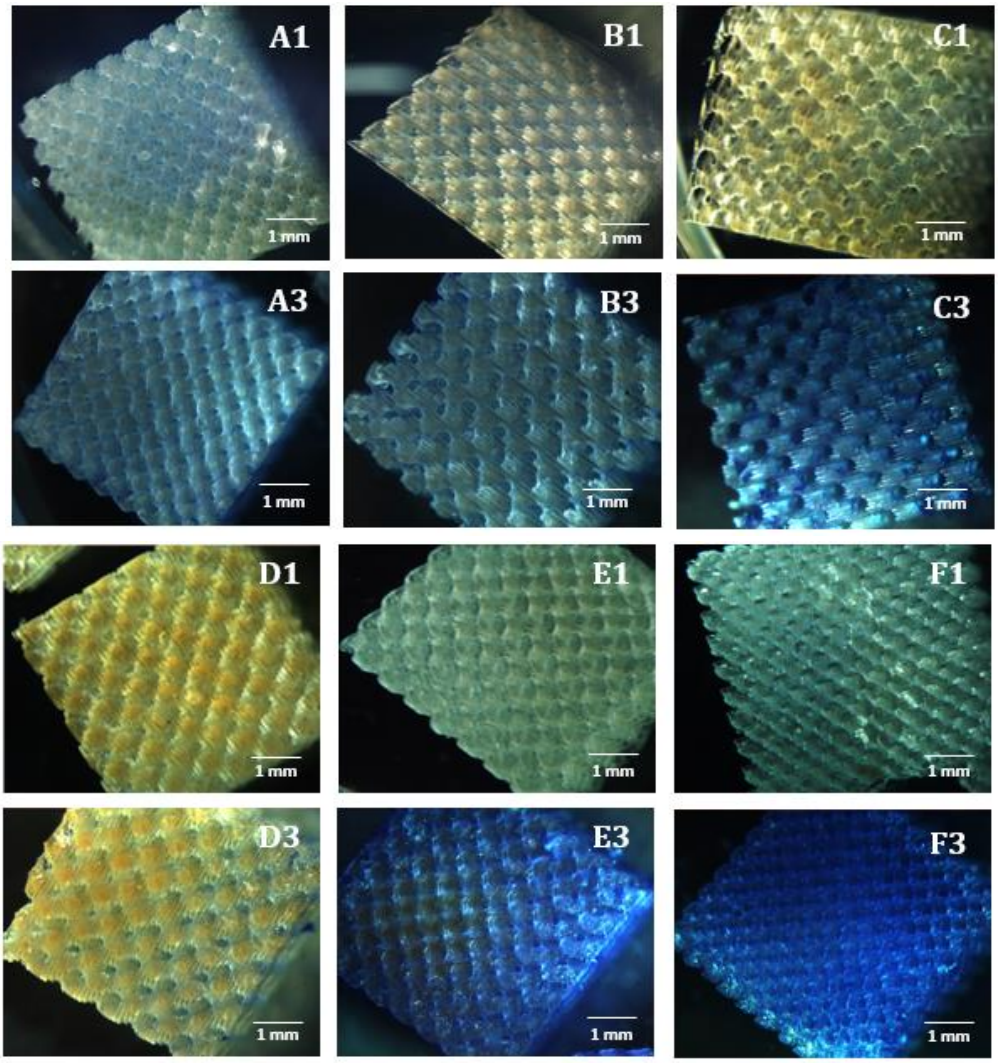

Figure 1 Cross-section stereomicroscope images of scaffolds for the constant surface area (A -311 µm; B - 394 µm; C - 493 µm) and pore size experiments (D -57 %, E-67 % and F-77 %). Cell adhesion and distribution with culture time (1- 24 hours of culture. 3 – 14 days of culture).

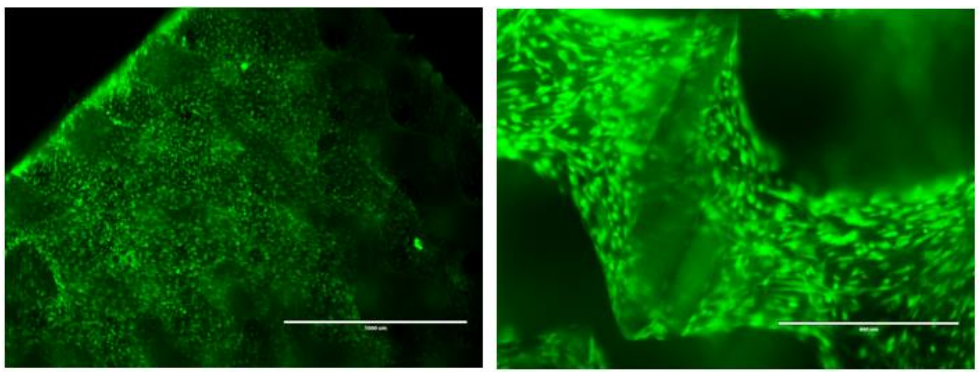

Figure 2 Live and Dead® fluorescence staining microscopic images. On the left: Formation of cell aggregates covering the outside of the 311 *µm* pore size scaffold after 14 days of culture: cells proliferate to the side of the scaffold from the bottom. On the Right: Oriented cells filling the scaffold's walls (493 µm pore size scaffold after 7 days of culture)

.

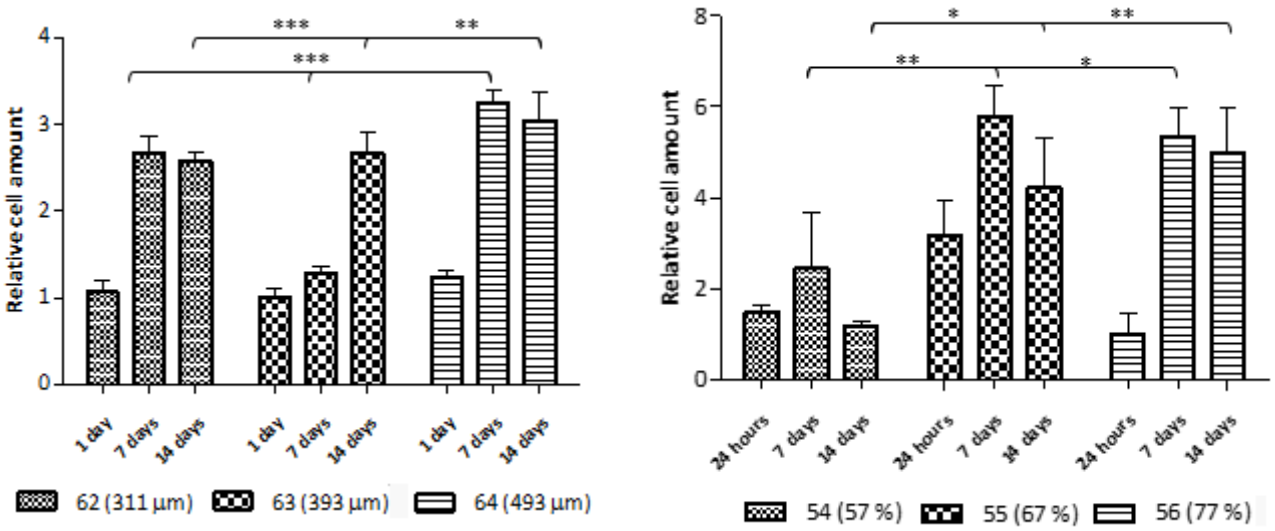

Figure 3 Relative cell amount for the scaffolds with constant surface area (7 μm^{-1}) on the left and constant pore size (430 μm) on the right, variation with time of culture under static conditions. The error bars correspond to the value of standard derivation of each sample. (In terms of statistical relevance *** corresponds to P<0.001;** to P< 0.01 and * to P< 0.05)

Higher amplifications reveal that the cells cultured in the *3D* environment of the PTMC scaffold, present a morphology corresponding to that described for the cells in the outer AF: ellipsoidal with long axes (Figure 2), meaning that there was not, loss of cell morphology. Proliferating cells appeared to be aligned (Figure 2), growing mainly in a perpendicular manner to the prototyped surface characterized by the stair-stepping effect. This effect seems to be beneficial, since the formed tortuous channels increased the residence time of cells inside the scaffold upon seeding and provided support for cell attachment and proliferation.

3.3 Cell seeding and culture

All constructs presented a tendency of cell growth overtime, with similar cell adhesion (Figure 3).

Better cell growth and proliferation was achieved, after 7 and 14 days of culture, for the larger pore size scaffold (493 μm). This reveals a tendency of increased cell amount for larger pore sizes, with statistically relevance (P<0.001) when compared to smaller pore size scaffolds (≤ 383 μm. This observation is consistent with the results previously obtained by Blanquer *et al* in 2013 [(2)]. These results are concordant with the ones obtained through methylene blue staining assay, corroborating the hypothesis that in constructs with larger pore sizes there's an eased diffusion of oxygen and nutrients to the cells present inside the scaffold that also enables the removal of harmful metabolites resultant from cellular activity. The final higher numbers of cells obtained for the 493 μm pore size constructs, can also be a consequence of initial cell behaviour, where the culture benefit from the fact that scaffold pores were only completely covered by in a later culture stage, promoting absence of cell aggregates, and improving cell migration as well as proliferation [(24), (25)]. Smaller pore size scaffolds (311 μm) presented cell aggregates, what in addition to poor nutrient diffusion may also have been responsible for the inhibition of cell growth, through intracellular signalling. This type of cell response has been previously reported for scaffolds with smaller pore sizes [(26)]. More importantly these narrower structures are not able to contain as many cells as the ones with larger pores, what can lead to insufficient ECM production and consequently alterations on the cell growth and behaviour [(26)].

The second experiment (Figure 3), revealed an increase of cell adhesion between the scaffolds with a porosity of 57 *%* and 67*%*. As mentioned before, increased porosity leads to a raise of the specific surface area. In fact, larger surface area

constructs have more space and a greater amount of ligands available for the attachment of cells [25]. However, between the constructs with higher porosities, from values of 67 % to 77 *%*, which also possess higher values of specific surface area, this tendency was not observed. This fact is intimately related with the scaffolds hydrophobicity and high porosity, which in seeding process causes the liquid cell suspension to pass through the scaffold. Furthermore, cells are easily detached from constructs with higher porosities and these may be washed-off before the DNA quantification procedure.

Analysing cell proliferation, scaffolds with higher porosities (≥ 67,0 *%*) exhibited higher amounts of cells after 7 and 14 days, when compared to the 57,0 *%* porosity scaffold (P<0.05). This demonstrates that higher values of porosity had improved cell proliferation rates and better cell distribution [25] [27] . However, the effect of the specific surface area and porosity on cell proliferation becomes less prominent for later culture times [25], and the 67 % and 77 % porosity scaffolds present comparable results for day 7 and 14 of culture, which is aligned with the studies by Rotman in 2013 [6]. High porosity and interconnection of pores is extremely important for diffusion of the nutrients from the medium, promoting cell growth and adequate ECM production. . As established in the first experiment (Table 1), scaffolds with higher porosity (74, 7 *%*) promote better cell proliferation. Therefore, it is not surprising that, after 14 days of culture, the 57% porosity scaffold presented a lower number of cells, being possible that the growth of cells around the scaffold has led growth arrest or even cell death. However no viability assay was performed to support such assumption.

3.4 Mechanical Properties

Determination of scaffold's mechanical properties is extremely significant regarding its applicability in tissue engineering. Due to PTMC's extreme elasticity [28], the compressed scaffolds were able to maintain their shape.

With regard to the scaffolds with cells, a growth trend tendency of the value of the compression moduli with time was observed, reaching from 0.299±0.089 *MPa* to 0.609±0.215 *MPa* after 14 days (Table 2). The increase in compression moduli observed was statistically significant (P<0.005), representing a rise of approximately 204 *%* from the initial value, probably due to the cell growth and increase of fibrous ECM production with culture time. Previous works showed increment of the compression moduli value with culture duration of bovine AF cells [22].

Table 2 Compression moduli of PTMC scaffolds determined for scaffolds with and without hAFC cells for different culture times. Values presented with the correspondent value of standard deviation.

	Time of culture (days)	State of scaffold	Compression modulus (MPa)
Scaffold without cells	-	Dry	0.21±0.03 [2]
	1	Wet	0.34±0.07
	7		0.28±0.09
	14		0.34±0.07
Scaffold with cells	1	Wet	0.30±0.09
	7		0.52±0.11
	14		0.61±0.22

The compression moduli achieved in the present study 0.609±0.215 *MPa*, fall into the range of natural human *annulus fib*rosus tissue (0.450-0.800 *MPa*) [2], [10], [21]. These are higher than the ones obtained by Blanquer *et al* [2] for dry PTMC scaffolds without cells, regardless of their pore size (230-420 *μm*). The results obtained in this study have a high impact, since they change the paradigm that smaller pore scaffolds are more suitable for tissue engineering of the AF [2], demonstrating that 7 to 14 days of cell culture is enough to raise the compression modulus the constructs made with larger pore size scaffolds. The improvement on the mechanical properties over culture time was also evident in the stress-strain compression curves obtained.

4 Conclusions

All the tested scaffolds presented good cell adhesion and proliferation, validating the use of PTMC made scaffolds for tissue engineering of the *annulus fib*rosus.

larger pore sizes (493 *μm*) and high porosities (≥ 67 %) were critical to promote high cell proliferation and uniform distribution, most

probably allowing proper nutrient diffusion to the inside of the scaffold and removal of toxic metabolites formed by normal cellular activity. Also, larger pores will initially provide better cell adhesion [(2)], and less cell aggregates formation [(27)] than smaller pores. The combination of high porosities and pore size diminishes the space in the construct occupied by scaffold's material therefore increasing the construct's percentage made of cells and ECM. This feature facilitates the regeneration process since cell and ECM densities close to the native tissue should be more easily achieved [(27)]. Higher cell proliferation was also promoted for scaffolds with higher specific surface area (≥ 7,36 μm^{-1}).

The porous PTMC constructs presented a significant maturation of their mechanical properties towards resembling with the native tissue features. Compression moduli increase over two times their initial value after 14 days of static culture (from 0.299±0.089 *MPa* to 0.609±0.215 *MPa*). This is critical for implantation of the tissue construct, which after such culture period, can be implanted providing the necessary mechanical support for cell growth, with no significant difference to the native tissue.

This study demonstrates that scaffolds designed and built with larger pore sizes (400 μm) are a better solution for repair of the AF tissue, compared to smaller pore size scaffolds (< 393 μm). The resulting constructs possess better cell distribution and proliferation, as well as more adequate mechanical performance, which can be responsible for the reduction of the recovery time of surgeries, once biofunctionality is readily achieved. Overall it was demonstrated that gyroid architecture PTMC scaffolds built using stereolithography hold a great potential for tissue engineering of the *annulus fib*rosus with possible re-establishment of the biomechanical function of the IVD.

5 Future Perspectives

Optimization of scaffold's design for application on tissue engineering of the *annulus fib*rosus is extremely challenging to achieve, since the several design parameters are dependent on each other.

We suggest that further studies with the already determined optimal conditions, should be conducted using dynamic culture in a bioreactor over longer periods of time, up to 6 months, to assess cell viability, extracellular matrix production, material degradation rates, mechanical properties maturation and effect of mechanical stimuli on gene expression and ECM production. Additional alterations to the scaffold's design, like application of a controlled pore size gradients [(29)], to mimic the structural differences between inner and outer AF should be considered as well as addiction or combination with different materials to deliver biologics or enhancing the constructs mechanical properties [(30)].

Overall, future research should include an adequate strategy for graft implantation and fixation *in vivo*, which ensures the functionality and viability of the engineered *annulus fib*rosus tissue.

6 Bibliographic References

1. *Lumbar Disc Disorders and Low-Back Pain: Socioeconomic Factors and Consequences.* **Katz, Jeffrey N.** 4, 2006 , J Bone Joint Surg Am, Vol. 88, pp. 21-24.

2. *Effect of Pore Characteristics on Mechanical Properties and Annulus Fibrous Cell Seeding and Proliferation in Designed PTMC Tissue Engineering Scaffolds.* **Blanquer, Sébastien B.G., et al.** s.l. : Wiley-VCH, 2013, Macromol. Symp., pp. 75-81.

3. *Annulus fibrosus tissue engineering using lamellar silk scaffolds.* **Park, Sang Hyug, et al.** s.l. : Wiley Online Publisher, 2012, Journal of Tissue Engineering and Regenerative Medicine, Vol. 6, pp. 24-33.

4. *Tissue engineering strategies applied in the regeneration of the human intervertebral disk.* **Silva-Correia, Joana, et al.** 8, 2013, Biotechnology advances, Vol. 31, pp. 1514-31.

5. *Intervertebral disc regeneration or repair with biomaterials and stem cell therapy - feasible or fiction?* **Chan, Scw and Gantenbein-Ritter, B.** May, s.l. : The European Journal of Medical Sciences , 2012, Swiss Medical Weekly, Vol. 142.

6. **S.G.Rotman.** *The effect of scaffolds characteristics on the growth of Annulus Fibrosus Cells.* Enschede : Universiteit Twente, 2013.

7. *Mechanobiology of the intervertebral Disc and Relevance to Disc Degeneration.* **Setton, Lori A. and Chen, Jun.** 2006, The Journal of Bone and Joint Surgery, Vol. 88, pp. 52-57.

8. *Repair, Regenerative and supportive theraphies of annulus fibrosus: achievements and challanges.* **Bron, Johanes L., Helder, Marco N. and Meisei, Hans-Jorg et all.** s.l. : Springer, 2009, European Spine Journal, Vol. 18, pp. 301-313.

9. *ISSLS prize winner: integrating theoretical and experimental methods for functional tissue engineering of the annulus fibrosus.* **Nerurkar, Nandan L, Mauck, Robert L and Elliott, Dawn M.** 25, s.l. : Lippincott Williams & Wilkins, 2008, Spine, Vol. 33, pp. 2691-2701.
10. *Challenges and strategies in the repair of ruptured annulus fibrosus.* **Guterl, C C, et al.** s.l. : Ecmjournal.org, 2013, European cells & materials, Vol. 25, pp. 1-21.
11. *The challenge and advancement of annulus fibrosus tissue engineering.* **Jin, Li, Shimmer, Adam L and Li, Xudong.** 5, s.l. : Springer, 2013, European Spine Journal , Vol. 22, pp. 1090-100.
12. **Likhitpanichkul, M., et al.** FIBRIN-GENIPIN ADHESIVE HYDROGEL FOR ANNULUS FIBROSUS REPAIR: PERFORMANCE EVALUATION WITH LARGE ANIMAL ORGAN CULTURE,IN SITU BIOMECHANICS, AND IN VIVO DEGRADATION TESTS. *European Cells and Materials.* 2014, Vol. 28, pp. 25-38.
13. *Shape-memory porous alginate scaffolds for regeneration of the annulus fibrosus: Effect of TGF-B3 supplementation and oxygen culture.* **Guillaume, Oliver, et al.** s.l. : Elsevier, 2014, Acta materialia, Vol. 10, pp. 1985-1995.
14. *Biodegradable Electrospun Scaffolds for Annulus Fibrosus Tissue Engineering: Effect of Scaffold Structure and Composition on Annulus Fibrosus Cells In Vitro.* **Grad, S., et al.** S01, s.l. : Tissue Engineering, 2012, Global Spine Journal, Vol. 2, pp. 672-82.
15. *Modulation of annulus fibrosus cell alignment and function on oriented nanofibrous polyurethane scaffolds under tension.* **Turner, Kathleen G., Ahmed, Nazish and Santerre, J. Paul and Kandel, Rita.** 3, s.l. : Elsevier, 2014, Spine Journal, Vol. 14, pp. 424-434.
16. *Translation of an engineered nanofibrous disc-like angly-ply structure for intervertebral disc replacement in a small animal model.* **Martin, John T, et al.** s.l. : Elsevier, 2014, Acta Biomaterial, Vol. 10, pp. 2473-2481.
17. *Nanofibrous biologic laminates replicate the form and function of the annulus fibrosus.* **Nerurkar, Nandan L., et al.** s.l. : Nature, 2009, Nature Materials, Vol. 8, pp. 986-992.
18. *Strategies for replicating anatomical cartilaginous tissue gradient in engineered intervertebral disc.* **Bhattacharjee, Maumita, et al.** 1, 2014, ACS applied materials & interfaces, Vol. 6, pp. 183-93.
19. *Porosity and Cell Preseeding Influence Electrospun Scaffold Maturation and Meniscus Integration In Vitro.* **Ionescu, Lara C. and Mauck, Robert L.** 3, s.l. : TISSUE ENGINEERING:, 2013, Vol. 19.
20. *The potential to improve cell infiltration in composite fiber-aligned electrospun scaffolds by the selective removal of sacrificial fibers.* **Baker BM, Gee AO, Metter RB, Nathan AS, Marklein RA, Burdick JA, Mauck RL.** 15, s.l. : Elsevier, 2008, Biomaterials, Vol. 29.
21. *Effects of the architecture of tissue engineering scaffolds on cell seeding and culturing.* **Melchels, Ferry P W, et al.** 11, s.l. : Elsevier, 2010, Acta Biomaterialia, Vol. 6, pp. 4208-4217.
22. *Flexible and Elastic Scaffolds for Cartilage Tissue Engineering Prepared by Stereolithography Using Poly(trimethylene carbonate)-Based Resins.* **Schuller-Ravoo, Sigrid, Feijen, Sandra M. Teixeira. Jan and Grijpma, Dirl W.** s.l. : Wiley Online, 2013, Macromolecular Bioscience, Vol. 13, pp. 1711-1719.
23. *Engineered three-dimensional nanofibrous multi-lamellar structure for annulus fibrosus repair.* **Kang, Ran, et al.** s.l. : RSCPublishing, 2013, Journal Materials Chemistry B, Vol. 1, pp. 5462-5468.
24. *The effect of pore size on cell adhesion in collagen-GAG scaffolds.* **O'Brien FJ, Harley BA, Yannas IV, Gibson LJ.** 4, s.l. : Elsevier, 2005, Biomaterials, Vol. 26, pp. 433-41.
25. *The effect of mean pore size on cell attachment, proliferation and migration in collagen-glycosaminoglycan scaffolds for bone tissue engineering.* **Murphy, Ciara M, Haugh, Matthew G and O'Brien, Fergal J.** 3, s.l. : Elsevier, 2010, Biomaterials, Vol. 31, pp. 461-6.
26. *Effect of pore size on ECM secretion and cell growth in gelatin scaffold for articular cartilage tissue engineering.* **Lien, Sio M., Ko, Liang Y. and Huang, Ta J.** 2, s.l. : Elsevier, 2009, Acta Biomaterialia, Vol. 5, pp. 670-679.
27. *Polymeric Scaffolds in Tissue Engineering Application: A Review.* **Dhandayuthapani, Brahatheeswaran, Yoshida, Yasuhiko and Maekawa, Toru and Kumar, D. Sakthi.** ii, s.l. : Hindawi Corporation , 2011, International Journal of Polymer Science, Vol. 2011, pp. 1-19.
28. *Advanced Microestructures based on Poly(trimethylene carbonate):.* **Schuller-Ravoo, Sigrid.** 2011.
29. *Three-dimensional plotted scaffolds with controlled pore size gradients: Effect of scaffold geometry on mechanical performance and cell seeding efficiency.* **Sobral, Jorge M, et al.** 3, s.l. : Elsevier, 2011, Acta biomaterialia, Vol. 7, pp. 1009-18.
30. *A review on stereolithography and its applications in biomedical engineering.* **Melchels, F. P W and Feijen, Jan: Grijpma, Dirk W.** 24, s.l. : Elsevier, 2010, Biomaterials, Vol. 31, pp. 6121-6130.